 CMES, vol.80, no.3, pp.201-217, 2011

Applicability of the Boundary Particle Method

F.Z. Wang[1,2,3]

Abstract: In this paper, we consider the boundary particle method (BPM) which is excellent in solving inhomogeneous partial differential equations in terms of solution accuracy and simplicity. In order to investigate the applicability of the BPM, we examine the relationship between its solution accuracy and the effective condition number. We show that the effective condition number, which estimates system stability with the right-hand side vector taken into account, is inversely proportional to the root mean square error in the numerical approximation. Moreover, for noisy-boundary cases, we find that the BPM can not yield reasonable results, for more noise added to the right-hand side vector, by using Gaussian elimination. Thus, to solve effectively the discrete ill-conditioned coefficient matrix, we adopt three regularization techniques under two different regularization parameter choices. Numerical results indicate that the generalized cross-validation choice rule for the damped singular value decomposition regularization strategy performs the best.

Keywords: Effective condition number, noisy-boundary, inhomogeneous, regularization technique, regularization parameter.

1 Introduction

Meshless methods have tremendously attracted many mathematicians and engineers in recent decades [Belytschko, Krongauz, Organ, Fleming, and Krysl (1996); Nguyen, Rabczuk, Bordas, and Duflot (2008); Ferreira, Kansa, Fasshauer, and Leitao (2009)]. It can be divided into two types, that is, domain-type meshless methods and boundary-type meshless methods.

Among the boundary-type meshless methods, the method of fundamental solutions [Fairweather and Karageorghis (1998); Chen, Karageorghis, and Smyrlis (2008)],

[1] College of Mathematics, Huaibei Normal University, No. 100 Dongshan Road, Huaibei, Anhui 235000, China

[2] Corresponding to: wangfuzhang@hhu.edu.cn

[3] Department of Engineering Mechanics, Hohai University, No.1 XiKang Road, Nanjing, Jiangsu 210098, China

the boundary node method [Mukherjee and Mukherjee (1997); Li, Huang, and Miao (2010)], the boundary knot method [Kang and Lee (2000); Chen and Hon (2003); Wang, Chen, and Jiang (2010)] and the desingularized meshless method [Young, Chen, and Lee (2005); Chen, Lu, and Hsu (2011)] are typically examples. These representative boundary-type meshless methods can solve homogeneous problems with boundary-only discretization, but require inner nodes in conjunction with the other techniques to handle inhomogeneous problems, take the dual reciprocity method (DRM) for example [Golberg (1995); Patridge, Brebbia, and Wrobel (1992)]. Similar to the DRM, the multiple reciprocity method (MRM) [Nowak and Neves (1994)] is another choice in dealing with inhomogeneous problems. The superior advantage of the MRM over the DRM lies in that the former does not need inner nodes for the particular solution in the process of solving inhomogeneous problems. To take advantage of its truly boundary-only merit, Chen [Chen (2002)] developed the MRM-based boundary particle method (BPM). The BPM is a meshless, integration-free strategy which uses either high-order nonsingular general solutions or singular fundamental solutions as the radial basis functions.

We note that the BPM produces a severely ill-conditioned full coefficient matrix when using a large number of boundary nodes, which is also encountered in the other boundary-type methods [Wang, Chen, and Jiang (2010); Chen, Chen, and Lee (2005); Liu (2008)]. Nevertheless, there often occurs the puzzle that the traditional L^2 condition number is extremely huge, but the approximate solutions are convincingly correct. Based on the L^2 condition number, such numerical solutions should be distrusted. Thus, an alternative measurement index called the effective condition number, which takes the right-hand side vector into account, was first introduced in [Christiansen and Hansen (1994)]. Recently, the relationship is studied between the effective condition number of a linear system and the solution accuracy when using the method of fundamental solutions [Drombosky, Meyer, and Ling (2009)] or the boundary knot method [Wang, Ling, and Chen (2009)]. However, if more noise is added to the right-hand side vector b, traditional methods like Gaussian elimination can not yield reasonable results. Thus, some regularization techniques has been investigated to obtain reasonable results [Wei, Hon, and Ling (2007); Ramachandran (2002); Chen, Hokwon, and Golberg (2006); Jin and Zheng (2005a); Jin and Zheng (2005b)].

In this paper, we first investigate the relationship between the solution accuracy and the effective condition number of a linear system when using the BPM. And then, we combine the BPM with various regularization techniques to examine Helmholtz problems under noisy-boundary conditions which are preferably for practical problems. Numerical experiments show that the Damped Singular Value Decomposi-

tion (DSVD) using the Generalized Cross-Validation (GCV) regularization parameter performs the best in terms of solution accuracy as well as stability.

2 BKM formulation

To briefly illustrate the BPM, we consider the following nonhomogeneous Helmholtz problem

$$\Delta u(X) + \lambda^2 u(X) = f(X) \qquad \text{in} \qquad \Omega \tag{1}$$

$$u(X) = \bar{u}(X) \qquad \text{on} \qquad \Gamma_1 \tag{2}$$

$$\frac{\partial u(X)}{\partial \bar{n}} = \bar{q}(X) \qquad \text{on} \qquad \Gamma_2 \tag{3}$$

where Δ represents the Laplacian, λ is the wave number, $\bar{n}$ the unit outward normal, u and q the potential and its normal derivative (flux), respectively. Ω stands for the solution domain in $\mathbb{R}^d$, where d denotes the dimensionality of the space, and $\partial\Omega(=\Gamma_1 \cup \Gamma_2)$ its boundary.

Using the superposition theorem, we can divide the solution of Eq. (1) into

$$u(X) = u_h^0(X) + u_p^0(X) \tag{4}$$

where $u_h^0(X)$ and $u_p^0(X)$ are the zero-order homogeneous and particular solutions, respectively. Using the MRM [Nowak and Neves (1994)], we can evaluate the particular solution in Eq. (4) by a sum of higher-order homogeneous solution $u_h^m(X)$, namely

$$u_p^0(X) = \sum_{m=1}^{\infty} u_h^m(X) \tag{5}$$

where the superscript m is the order index of homogeneous solution. Thus, the solution of inhomogeneous equation Eq. (1) can be rewritten as

$$u(X) = u_h^0(X) + u_p^0(X) = \sum_{m=0}^{\infty} u_h^m(X) \tag{6}$$

On the other hand, the zero-order homogeneous solution $u_h^0(x)$ has to satisfy both the governing equation and the boundary conditions, i.e.

$$L\{u_h^0(X)\} = 0 \qquad \text{in} \quad \Omega \tag{7}$$

$$u_h^0(X) = \bar{u}(X) - u_p^0(X) \qquad \text{on} \quad \Gamma_1 \tag{8}$$

$$\frac{\partial u_h^0(X)}{\partial \bar{n}} = \bar{q}(X) - \frac{\partial u_p^0(X)}{\partial \bar{n}} \qquad \text{on} \quad \Gamma_2 \tag{9}$$

where L indicates the Helmhotz operator $\triangle + \lambda^2$. Eqs. (8) and (9) are in fact the DRM formula without using inner nodes [Nowak and Neves (1994)]. In contrast, the MRM also involves the higher order homogeneous solution. Through a similar incremental differentiation operation over Eqs. (8) and (9) via operator $L\{\cdot\}$, we have successive higher order boundary differential equations

$$L^{n-1}\{u_h^0(X)\} = L^{n-2}\{f(X)\} - L^{n-1}\{u_p^n(X)\} \quad \text{on} \quad \Gamma_1 \tag{10}$$

$$\frac{\partial L^{n-1}\{u_h^n(X)\}}{\partial \bar{n}} = \frac{\partial (L^{n-2}\{f(X)\} - L^{n-1}\{u_p^n(X)\})}{\partial \bar{n}} \quad \text{on} \quad \Gamma_2 \tag{11}$$

where $L^0\{f(x)\} = f(x)$ and $L^m\{\cdot\} = L^{m-1}\{L\{\cdot\}\} = \cdots = L\{L\{L\{L\{\cdots\}\}\}\}$ denotes the m-th order operator of $L\{\cdot\}$ with $m \geq 1$. The n-th order homogeneous solution can be approximated by

$$u_h^n(X) = \sum_{k=1}^{N} \beta_k^n u_n^*(r_k) \tag{12}$$

where N is the number of boundary nodes, k the index of source nodes on boundary, β_k the desired coefficients, and $r_k = \| X - X_k \|$ the Euclidean distance norm. $u_n^*(\cdot)$ represents the fundamental solution or the nonsingular general solution of operator $L^n\{\cdot\}$. Like the MFS, the usage of fundamental solutions requires a fictitious boundary outside the physical domain. Therefore, we use the nonsingular general solution rather than the fundamental solution in this paper.

Collocating Eqs. (8)-(11) at all boundary nodes in terms of the representation (12), we have the BPM boundary discretization equations:

$$\sum_{k=1}^{N} \beta_k^0 u_0^*(r_{ik}) = \bar{u}(x) - u_p^0(x_i) \tag{13}$$

$$\sum_{k=1}^{N} \beta_k^0 u_0^*(r_{jk}) = \bar{q}(x) - \frac{\partial u_p^0(x_j)}{\partial \bar{n}} \tag{14}$$

$$\sum_{k=1}^{N} \beta_k^1 u_n^*(r_{ik}) = L^{n-2}\{f(x_i)\} - L^{n-1}\{u_p^n(x_i)\} \tag{15}$$

$$\sum_{k=1}^{N} \beta_k^1 u_n^*(r_{jk}) = \frac{\partial (L^{n-2}\{f(x_j)\} - L^{n-1}\{u_p^n(x_j)\})}{\partial \bar{n}} \tag{16}$$

As in the MR-BEM [Nowak and Neves (1994)], the successive process is truncated at some order M, namely,

$$L^{M-1}\{u_p^M\} = 0. \tag{17}$$

The practical solution procedure is a reversal recursive process:

$$L^M \to L^{M-1} \to \cdots \to L^0. \tag{18}$$

It is noted that due to

$$L^{n-1}\{u_n^*(r)\} = u_0^*(r), \tag{19}$$

the coefficient matrices of all successive equations (13)-(16) are the same, i.e.

$$A\beta^n = b^n, \qquad n = M, M-1, \cdots 1, 0. \tag{20}$$

The LU decomposition algorithm is suitable for this task. We can employ the obtained expansion coefficients β to calculate the BPM solution at any node, i.e.

$$u(X_i) = \sum_{n=0}^{M} \sum_{k=1}^{N} \beta_k^n u_n^*(r_{ik}). \tag{21}$$

For more details, we refer readers to [Chen (2002)].

We find that being a global interpolation approach, the BPM produces an ill-conditioned coefficient matrix, especially when using a large number of boundary nodes, which is clearly reflected by its associated huge L^2 condition number. It is worthy noting that the L^2 condition number measures the conditioning of coefficient matrix by a ratio of the maximum and minimum eigenvalues of the coefficient matrix A. The *fixed* vector b in the right-hand side of equation

$$A\alpha = b \tag{22}$$

is not considered in the L^2 condition number. As an alternative measurement index, the effective condition number is introduced to include the effect of vector b [Drombosky, Meyer, and Ling (2009)]. More details are given in the next section.

3 Measurement of the coefficient matrix conditioning

As is known to all, the coefficient matrix A in Eq. (22) can be decomposed as

$$A = U\Sigma V^T, \tag{23}$$

where $U = [u_1, u_2, \cdots, u_N]$ and $V = [v_1, v_2, \cdots, v_N]$ are orthogonal matrices, $U^T U = V^T V = I_N$, where I_N denotes the identity matrix and Σ is a diagonal matrix with diagonal elements

$$\sigma_1 \geq \sigma_2 \geq \cdots \geq \sigma_N > 0, \tag{24}$$

where $\sigma_i, 1 \leq i \leq N$ are called singular values of A while the vectors u_i and v_i are the left and right singular vectors of A, respectively.

Such a process is referred to as the singular value decomposition. The L^2 condition number of a nonsingular square matrix A is defined by $\text{Cond}(A) = \| A \| \cdot \| A^{-1} \|$, where the matrix $2-$norm is used throughout this paper, the L^2 condition number can be stated as $\text{Cond}(A) = \sigma_1/\sigma_n$, where σ_1 and σ_n are the largest and smallest singular value of A, respectively.

Substituting Eq.(23) into Eq.(22), we have

$$\alpha = \sum_{i=1}^{N} \frac{u_i^T b}{\sigma_i} v_i. \tag{25}$$

For practical applications, the boundary data b may be disturbed by some noise. Clearly, we should not rely solely on the L^2 condition number to predict accuracy of the computed solution of all practical ill-conditioned BPM systems. Most importantly, the solution accuracy of the BPM has an obvious dependence on the right-hand side vector. Since the L^2 condition number does not involve the right-hand side vector b, any research of the system stability irrelevant to the choice of b is not appropriate. In many applications, b is problem-dependent but fixed. Under these conditions, as an alternative tool to estimate the solution accuracy of the BPM, we consider the effective condition number $\text{ECN} = \text{ECN}(A, b)$, which is defined as follows [Drombosky, Meyer, and Ling (2009)].

Consider a perturbed matrix system $A(\alpha + \triangle\alpha) = b + \triangle b$. From which we can derive

$$b = \sum_{i=1}^{N} \xi_i u_i, \quad \triangle b = \sum_{i=1}^{N} \triangle\xi_i u_i. \tag{26}$$

Let $\xi = (b_1, ..., b_N)^T = U^* b$ and $\triangle\xi = (\triangle b_1, ..., \triangle b_N)^T = U^* \triangle b$. The solution can be expressed in terms of the inverse of A, namely

$$\alpha = A^{-1} b := V \Sigma^{-1} U^T b, \quad \triangle\alpha = A^{-1} \triangle b. \tag{27}$$

Suppose $p \leq N$ is the largest integer such that $\sigma_p > 0$, that is

$$\Sigma^{-1} = \text{Diag}(\sigma_1^{-1}, ..., \sigma_p^{-1}, 0, ..., 0). \tag{28}$$

Since U is orthogonal, we have

$$\| \alpha \| = \sqrt{\sum_{i=1}^{N} (\frac{\xi_i}{\sigma_i})^2}, \quad \| \triangle\alpha \| = \sqrt{\sum_{i=1}^{N} (\frac{\triangle\xi_i}{\sigma_i})^2} \leq \frac{\| \triangle b \|}{\sigma_N}. \tag{29}$$

If both $A\alpha = b$ and $A(\alpha + \triangle\alpha) = b + \triangle b$ exist, then

$$\frac{\| \triangle\alpha \|}{\alpha} \leq \mathrm{Cond}(A) \frac{\| \triangle b \|}{b}. \tag{30}$$

Substituting Eq.(29) into the inequality (30) results in a new error bound for Eq.(22) with the ECN, as an alternative replacement of L^2 condition number

$$\mathrm{ECN}(A,b) = \frac{\| b \|}{\sigma_N \sqrt{\left(\frac{\xi_1}{\sigma_1}\right)^2 + \ldots + \left(\frac{\xi_N}{\sigma_N}\right)^2}}. \tag{31}$$

For other types of ECN, we refer readers to Christiansen and Hansen (1994); Li, Chien, and Huang (2007); Banoczi, Chiu, Cho, and Ipsen (1998).

4 Regularization methods

Based on the singular value decomposition, we briefly present three commonly used regularization techniques under two parameter choices, that is, the TSVD, the Tikhonov regularization (TR) and the Damped Singular Value Decomposition (DSVD) under parameter choice of the *L*-curve criterion (LC) and the GCV Wei, Hon, and Ling (2007); Hansen (1994).

4.1 Regularization techniques for discrete problems

TSVD: The TSVD solution is often used to obtain a better estimate of the least squares solution. It is given by approximating a rank$-N$ full matrix A by a rank K matrix in which only the largest K singular values are retained

$$A_K = \sum_{i=1}^{K} u_i \sigma_i v_i^T. \tag{32}$$

In this instance, we can replace matrix A in Eq. (22) by A_K, which has a well defined null space of dimension $N-K$ spanned by the right singular value vectors, $v_{K+1}, \ldots, v_N$. The original linear system Eq. (22) is then replaced by the following problem set of Eq. (33), where b is ideal noise-free data obtained at the minimized node. The resulting TSVD solution of

$$\min\|\alpha\|_2 \quad \text{is} \quad \text{subject} \quad \text{to} \quad \min\|A_K\alpha - b\|_2 = \min \tag{33}$$

is given by

$$\alpha_K = \sum_{i=1}^{K} \frac{u_i^T b}{\sigma_i} v_i \tag{34}$$

where $K \leq N$ is also a regularization parameter.

TR: The TR replaces the linear system (22) by the minimization problem

$$\min_{\alpha \in R^n} \|A\alpha - b\|^2 + \mu^2 \|\alpha\|^2 \tag{35}$$

where $\mu \geq 0$ is a regularization parameter.

Based on the singular value decomposition, we can express Eq. (35) in terms of

$$\alpha_\mu = \alpha_{\mathbf{min}} = \sum_{i=1}^{l} f_i \frac{u_i^T b}{\sigma_i} v_i \tag{36}$$

where l is the rank of matrix A and the Wiener weights are

$$f_i = \frac{\sigma_i^2}{\sigma_i^2 + \mu^2}. \tag{37}$$

DSVD: A relatively less known regularization technique which is based on the singular value decomposition is the DSVD. Here, instead of using the filter factors (37) in the TR, one introduces a smoother cut-off by means of filter factors f_i defined as

$$f_i = \frac{\sigma_i}{\sigma_i + \mu} \tag{38}$$

these filter factors decay slower than the Tikhonov filter factors and thus, in a sense, introduces less filtering.

The suitable value of the regularization parameter $\mu \geq 0$ is chosen by the LC or the GCV in this paper.

4.2 Regularization parameters

The appropriate value choice for the regularization parameter μ remains an open problem till now [Wang, Chen, and Jiang (2010)]. Here, we briefly introduce the LC criterion and the GCV parameter choice [Hon and Wei (2005); Turco (1998)].

LC for Choosing the Regularization Parameter: The LC is defined as

$$L := \{(\log\|\alpha_\mu\|, \log\|A\alpha_\mu - b\|) : \mu \geq 0\}. \tag{39}$$

Note here that the L-curve is a continuous curve when the regularization parameter is real in the TR and the DSVD. In numerical computation, the node with maximum curvature will be searched as the corner of the L-curve. For the discrete one, such as in TSVD, a finite set of nodes

$$\{(\log\|\alpha_q\|, \log\|A\alpha_q - b\|) : q = 1, 2, ..., N\} \tag{40}$$

will be obtained and interpolated by a spline curve. The node on the spline curve with the maximum curvature is then chosen as the desirable regularization parameter.

The distinctive feature of the LC lies in that the regularized solution varies with the regularization parameter μ.

GCV for Choosing the Regularization Parameter: The GCV is a statistical method which estimates the optimal value of the regularization parameter, by minimizing the functional

$$V(K) = \frac{\frac{1}{N}\|(I - A(K))b\|^2}{[\frac{1}{N}\text{trace}(I - A(K))]^2} \tag{41}$$

where $A(K)$ is defined as follows:

$$A\alpha_K = A(K)b \tag{42}$$

The GCV is a predictive mean-square error criteria, in the sense that it estimates the minimizer of residual function

$$T(K) = \frac{1}{N}\|A(\alpha_K - \alpha)\|^2 \tag{43}$$

In the following section, as a comparison to the BPM with no regularization technique, numerical results are given by using six regularization methods, that is, GCV-TR, LC-TR, GCV-DSVD, LC-DSVD, GCV-TSVD and LC-TSVD.

5 Numerical Examples

We consider three numerical cases for inhomogeneous Helmholtz problems. Some random noise to the boundary conditions is added by

$$u = \overline{u} + \delta, \quad q = \overline{q} + \delta \tag{44}$$

where $\delta = \varepsilon \times \text{Rand}$. We use the uniform random number generator to produce random numbers Rand in $[-1, 1]$. Here, ε denotes the noise level. The *root mean square error* in the following tables is defined as [Wang, Chen, and Jiang (2010)]

$$\text{RMSE} = \sqrt{\frac{1}{N_t}\sum_{j=1}^{N_t} |\frac{u(X_j) - \tilde{u}(X_j)}{u(X_j)}|^2} \tag{45}$$

for $|u(X_j)| \geq 10^{-3}$

$$\text{RMSE} = \sqrt{\frac{1}{N_t}\sum_{j=1}^{N_t} |u(X_j) - \tilde{u}(X_j)|^2} \tag{46}$$

for $|u(X_j)| < 10^{-3}$, where j is the index of test nodes we are interested in, $u(x_j)$ and $\tilde{u}(x_j)$ are the exact and numerical solutions respectively, and N_t denotes the total tested node number.

For the following three cases, we consider the inhomogeneous Helmholtz equation

$$\Delta u(x,y) + \lambda^2 u(x,y) = 2\sin(x)\cos(y) + 4\omega x\cos(x)\cos(y) \tag{47}$$

with corresponding wave number $\lambda = \sqrt{2}$ [Chen (2002)].

5.1 Square domain case

In this case, we analyze the inhomogeneous Helmholtz equation (47) on an unit square domain with only Dirichlet boundary condition. Analytical solution is given by

$$u = x^2\sin(x)\cos(y). \tag{48}$$

The coefficient matrix A is solely determined by the positioning of the boundary nodes, while the right-hand side vector is determined by the boundary data and the imposed noise level. Thus, the noise will only affect the right-hand side vector b rather than the BPM coefficient matrix.

Table 1: Case 1: Boundary node number $N = 60$.

Noise level	Cond	ECN	RMSE
0.0	2.87×10^{20}	3.62×10^{9}	9.32×10^{-5}
0.00001	2.87×10^{20}	1.97×10^{5}	9.60×10^{-3}
0.00005	2.87×10^{20}	2.12×10^{4}	7.84×10^{-2}
0.0001	2.87×10^{20}	2.35×10^{4}	7.16×10^{-2}
0.0005	2.87×10^{20}	2.77×10^{3}	2.61×10^{-1}
0.001	2.87×10^{20}	2.28×10^{3}	1.41×10^{-1}
0.005	2.87×10^{20}	4.53×10^{2}	2.92×10^{0}

It is seen from Table 1 that the ECN decreases with more noise added, while the RMSE performs contrarily. We observe a vertical increase in the ECN as a tiny amount of noise $\varepsilon = 0.00001$ is added. Even though all runs in Table 1 have exactly the same L^2 condition number, we observe completely different error behaviors in cases with higher noise levels.

The data in Table 1 strongly support the relation ECN $= o(\text{RMSE}^{-1})$. As more noise is added, the ECN is small enough to indicate that the BPM solution will not

be of machine epsilon accuracy. Since only the right-hand vector b is altered, this example can be considered as an appropriate starting point to show the relationship between the solution accuracy of the BPM and the ECN. All else stays constant, including the ill-conditioned coefficient matrix A. On the other hand, the small ECN found in Table 1 suggests that numerical solutions are not reliable once the noise $\varepsilon = 0.005$ is added. Thus, we adopt regularization methods instead of applying BPM directly under such cases.

Table 2: Case 1: Boundary node number $N = 60$ and noise level $\varepsilon = 0.005$.

Methods	ECN	RMSE
LC-TR	4.53×10^2	4.08×10^{-4}
LC-DSVD	4.53×10^2	3.89×10^{-5}
LC-TSVD	4.53×10^2	2.70×10^{-2}
GCV-TR	4.53×10^2	3.59×10^{-5}
GCV-DSVD	4.53×10^2	3.36×10^{-5}
GCV-TSVD	4.53×10^2	2.86×10^{-5}

For fixed noise level $\varepsilon = 0.005$ and boundary node number $N = 60$, Table 2 shows the RMSE by using six regularization methods. We observe that the GCV-DSVD gives the best solution accuracy with RMSE $= 2.86 \times 10^{-5}$, while the LC-TSVD gives the worst one with RMSE $= 2.70 \times 10^{-2}$.

5.2 Irregular domain case

Next, we consider the inhomogeneous Helmholtz equation as described in Case 1, but under a complex-shaped geometric domain which is sketched in Fig. 1.

The relationship between the ECN and the BPM solution accuracy is shown in Table 3. From which we can see that the relation ECN $= o(\text{RMSE}^{-1})$ still holds for complex-shaped geometry problems. Although all results in Table 3 have exactly the same L^2 condition number, we observe completely different error behaviors for various noise levels. For the noise-free boundary case, the ECN is of the order 10^9 even though the L^2 condition number is one order smaller than that in Case 1. Once again, we see the drop in both ECN and maximum error once $\varepsilon = 0.00001$ of noise is added.

For fixed noise level $\varepsilon = 0.005$ and the boundary node number $N = 68$, Table 4 gives the solution accuracy in terms of the RMSE by using six regularization methods. From which we can see that all regularization methods perform very well with order 10^{-6} except the LC-TSVD. We observe that the GCV-DSVD performs

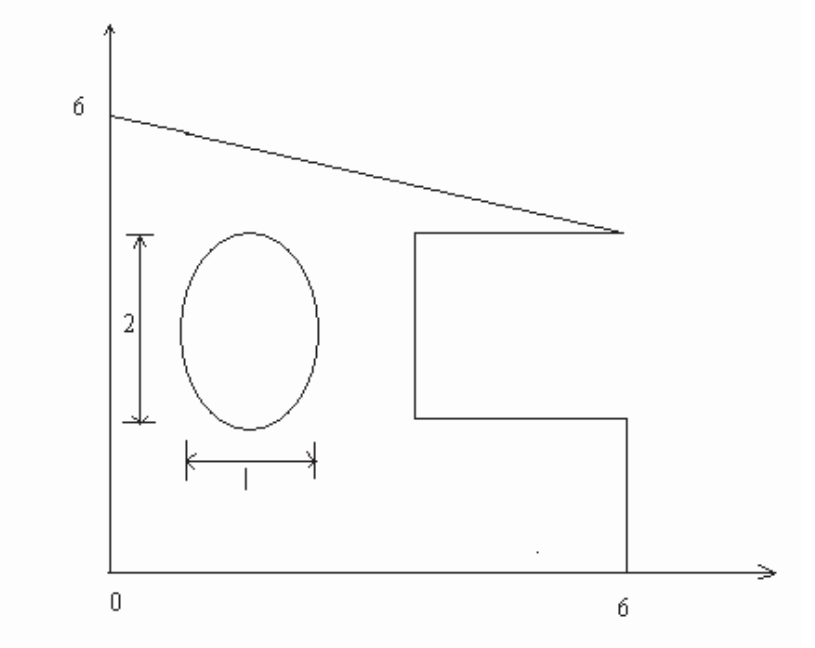

Figure 1: Irregular geometry for Case 2

the best with RMSE $= 3.49 \times 10^{-6}$, while the LC-TSVD performs the worst one with RMSE $= 1.16 \times 10^{-5}$.

5.3 Mixed boundary case with medium wave number

To more precisely illustrate the relationship between the ECN and the BPM solution accuracy, we reconsider the inhomogeneous Helmholtz equation (47) but under the irregular geometry depicted in Fig. 1, which involves mixed boundary conditions, namely, two adjacent Neumann edges $(x = 0, y = 0)$ and the rest Dirichlet edge. Analytical solution is given by

$$u = x^2 \sin(\lambda x)\cos(\lambda y) \tag{49}$$

with corresponding wave number $\lambda = 20$.

For fixed boundary node number $N = 82$, Table 5 describes variation of the ECN and the RMSE versus the increasing noise level. Also, we see the drop in both ECN and maximum error once $\varepsilon = 0.00001$ of noise is added. Using the observations in Table 5, we can conclude that the numerical approximation will agree with the exact solution up to about one decimal place with noise level $\varepsilon = 0.005$, which is enough for solving many engineering problems.

Table 3: Case 2: Boundary node number $N = 68$.

Noise level	Cond	ECN	RMSE
0.0	5.22×10^{19}	9.39×10^{9}	7.31×10^{-5}
0.00001	5.22×10^{19}	5.82×10^{5}	3.60×10^{-3}
0.00005	5.22×10^{19}	1.45×10^{5}	1.80×10^{-3}
0.0001	5.22×10^{19}	1.40×10^{4}	1.66×10^{-2}
0.0005	5.22×10^{19}	3.28×10^{3}	6.37×10^{-2}
0.001	5.22×10^{19}	1.76×10^{4}	5.53×10^{-2}
0.005	5.22×10^{19}	8.25×10^{2}	2.32×10^{0}

Table 4: Case 2: Boundary node number $N = 68$ and noise level $\varepsilon = 0.005$.

Methods	ECN	RMSE
LC-TR	8.25×10^{2}	9.35×10^{-6}
LC-DSVD	8.25×10^{2}	6.53×10^{-6}
LC-TSVD	8.25×10^{2}	1.16×10^{-5}
GCV-TR	8.25×10^{2}	3.58×10^{-6}
GCV-DSVD	8.25×10^{2}	3.49×10^{-6}
GCV-TSVD	8.25×10^{2}	3.73×10^{-6}

For the one decimal solution accuracy of noise level $\varepsilon = 0.005$, we analyze the RMSE by using six regularization methods whose results are shown in Table 6. We find that the GCV-DSVD is superior to the other regularization methods with RMSE $= 9.70 \times 10^{-3}$, but the LC-TSVD almost give unreasonable result with RMSE $= 1.07 \times 10^{5}$ to this case. Although the TSVD under parameter choice of the LC is effective for solving inverse problems with noisy-boundary conditions Wei, Hon, and Ling (2007); Hon and Wei (2005), it fails to yield acceptable numerical approximation here.

6 Conclusions

To investigate applicability of the boundary particle method, we introduce the ECN and analyze the relationship between the BPM solution accuracy and the ECN. Numerical results show that the effective condition number, which estimates system stability with the right-hand side vector taken into account, is inversely proportional to the RMSE in the numerical approximation.

It is also noted that for more noise added to the right-hand side vector, the BPM can

Table 5: Case 3: Boundary node number $N = 82$.

Noise level	Cond	ECN	RMSE
0.0	1.09×10^{19}	2.67×10^{9}	1.42×10^{-4}
0.00001	1.09×10^{19}	2.19×10^{6}	6.40×10^{-3}
0.00005	1.09×10^{19}	1.28×10^{5}	6.70×10^{-3}
0.0001	1.09×10^{19}	1.37×10^{4}	3.02×10^{-2}
0.0005	1.09×10^{19}	1.00×10^{4}	2.54×10^{-2}
0.001	1.09×10^{19}	3.67×10^{3}	1.26×10^{-1}
0.005	1.09×10^{19}	1.48×10^{3}	2.77×10^{-1}

Table 6: Case 3: Boundary node number $N = 82$ and noise level $\varepsilon = 0.005$.

Methods	ECN	RMSE
LC-TR	1.48×10^{3}	3.99×10^{-2}
LC-DSVD	1.48×10^{3}	2.41×10^{-2}
LC-TSVD	1.48×10^{3}	1.07×10^{5}
GCV-TR	1.48×10^{3}	9.80×10^{-3}
GCV-DSVD	1.48×10^{3}	9.70×10^{-3}
GCV-TSVD	1.48×10^{3}	3.65×10^{-2}

not yield reasonable results by using Gaussian elimination. Thus, three regularization techniques under two different regularization parameter choices are introduced to seek for improvement. From the above-tested three numerical examples, we conclude that the GCV choice ruler for the DSVD regularization method performs the best in terms of solution accuracy and stability.

Based on this study, one can use the ECN to determine if the BPM is a feasible method for solving the partial differential equation in hand. Meanwhile, one can use the DSVD under parameter choice of the GCV to solve problems with ill-conditioned coefficient matrix. Moreover, there is much theoretical investigation that needs to be done in this area of numerical analysis.

Acknowledgement: The work described in this paper was supported by a research project funded by Huaibei Normal University (Project No. 600571).

References

Banoczi, J. M.; Chiu, N. C.; Cho, G. E.; Ipsen, I. C. F. (1998): The lack of influence of the right-hand side on the accuracy of linear system solution. *SIAM: SIAM Journal on Scientific Computing*, vol. 20, no. 1, pp. 203–227.

Belytschko, T.; Krongauz, Y.; Organ, D.; Fleming, M.; Krysl, I. (1996): Meshless methods: An overview and recent developments. *Computer Methods in Applied Mechanics and Engineering*, vol. 139, no. 1-4, pp. 3–47.

Chen, C. S.; Hokwon, A. C.; Golberg, M. A. (2006): Some comments on the ill-conditioning of the method of fundamental solutions. *Engineering Analysis with Boundary Elements*, vol. 30, no. 5, pp. 405–410.

Chen, C. S.; Karageorghis, A.; Smyrlis, Y. S. (2008): *The Method of Fundamental Solutions - A Meshless Method*. Dynamic Publishers.

Chen, J. T.; Chen, I. L.; Lee, Y. T. (2005): Eigensolutions of multiply-connected membranes using method of fundamental solution. *Engineering Analysis with Boundary Elements*, vol. 29, no. 2, pp. 166–174.

Chen, K. H.; Lu, M. C.; Hsu, H. M. (2011): Regularized meshless method analysis of the problem of obliquely incident water wave. *Engineering Analysis with Boundary Elements*, vol. 35, no. 3, pp. 355–362.

Chen, W. (2002): Meshfree boundary particle method applied to helmholtz problems. *Engineering Analysis with Boundary Elements*, vol. 26, no. 7, pp. 577–581.

Chen, W.; Hon, Y. C. (2003): Numerical investigation on convergence of boundary knot method in the analysis of homogeneous helmholtz, modified helmholtz and convection-diffusion problems. *Computer Methods in Applied Mechanics and Engineering*, vol. 192, no. 15, pp. 1859–1875.

Christiansen, S.; Hansen, P. C. (1994): The effective condition number applied to error analysis of certain boundary collocation methods. *Journal of Computational and Applied Mathematics*, vol. 54, no. 1, pp. 15–36.

Drombosky, T. W.; Meyer, A. L.; Ling, L. (2009): Applicability of the method of fundamental solutions. *Engineering Analysis with Boundary Elements*, vol. 33, no. 5, pp. 637–643.

Fairweather, G.; Karageorghis, A. (1998): The method of fundamental solutions for elliptic boundary value problems. *Advances in Computational Mathematics*, vol. 9, no. 1, pp. 69–95.

Ferreira, A. J. M.; Kansa, E. J.; Fasshauer, G. E.; Leitao, V. M. A. (2009): *Progress on Meshless Methods*. Springer.

Golberg, M. (1995): The method of fundamental solutions for poisson's equation. *Engineering Analysis with Boundary Elements*, vol. 16, no. 3, pp. 205–213.

Hansen, P. (1994): Regularization tools: A matlab package for analysis and solution of discrete ill-posed problems. *Numerical Algorithms*, vol. 6, no. 1, pp. 1–35.

Hon, Y. C.; Wei, T. (2005): The method of fundamental solution for solving multidimensional inverse heat conduction problems. *CMES: Computer Modeling in Engineering & Sciences*, vol. 7, no. 2, pp. 119–132.

Jin, B. T.; Zheng, Y. (2005): Boundary knot method for some inverse problems associated with the helmholtz equation. *International Journal for Numerical Methods in Engineering*, vol. 62, no. 12, pp. 1636–1651.

Jin, B. T.; Zheng, Y. (2005): Boundary knot method for the cauchy problem associated with the inhomogeneous helmholtz equation. *Engineering Analysis with Boundary Elements*, vol. 29, no. 10, pp. 925–935.

Kang, S. W.; Lee, J. M. (2000): Eigenmode analysis of arbitrarily shaped two-dimensional cavities by the method of point matching. *Journal of the Acoustical Society of America*, vol. 107, no. 3, pp. 1153–1160.

Li, K.; Huang, Q. B.; Miao, Y. (2010): Dual reciprocity hybrid boundary node method for acoustic eigenvalue problems. *Engineering Analysis with Boundary Elements*, vol. 34, no. 4, pp. 359–368.

Li, Z. C.; Chien, C. S.; Huang, H. T. (2007): Effective condition number for finite difference method. *Journal of Computational and Applied Mathematics*, vol. 198, no. 1, pp. 208–235.

Liu, C. S. (2008): Improving the ill-conditioning of the method of fundamental solutions for 2d laplace equation. *CMES: Computer Modeling in Engineering & Sciences*, vol. 28, no. 2, pp. 77–93.

Mukherjee, Y. X.; Mukherjee, S. (1997): The boundary node method for potential problems. *International Journal for Numerical Methods in Engineering*, vol. 40, no. 5, pp. 797–815.

Nguyen, V. P.; Rabczuk, T.; Bordas, S.; Duflot, M. (2008): Meshless methods: A review and computer implementation aspects. *Mathematics and Computers in Simulation*, vol. 79, no. 3, pp. 763–813.

Nowak, A. J.; Neves, A. C. (1994): *The multiple reciprocity boundary element method*. Computational Mechanics Publication.

Patridge, P. W.; Brebbia, C. A.; Wrobel, L. W. (1992): *The dual reciprocity boundary element method*. Computational Mechanics Publication.

Ramachandran, P. (2002): Method of fundamental solutions: singular value decomposition analysis. *Communications in Numerical Methods in Engineering*, vol. 18, no. 11, pp. 789–801.

Turco, E. (1998): Load distribution modelling for pin-jointed trusses by an inverse approach. *Computer Methods in Applied Mechanics and Engineerings*, vol. 165, no. 1-4, pp. 291–306.

Wang, F. Z.; Chen, W.; Jiang, X. R. (2010): Investigation of regularized techniques for boundary knot method. *International Journal for Numerical Methods in Biomedical Engineering*.

Wang, F. Z.; Ling, L.; Chen, W. (2009): Effective condition number for boundary knot method. *CMC: Computers Materials & Continua*, vol. 12, no. 1, pp. 57–70.

Wei, T.; Hon, Y. C.; Ling, L. (2007): Method of fundamental solutions with regularization techniques for cauchy problems of elliptic operators. *Engineering Analysis with Boundary Elements*, vol. 31, no. 3, pp. 373–385.

Young, D. L.; Chen, K. H.; Lee, C. W. (2005): Novel meshless method for solving the potential problems with arbitrary domains. *Journal of Computational Physics*, vol. 209, no. 1, pp. 290–321.